powders

MDPI

Article

The Influence of Boron Additions on Sintering and Mechanical Properties of WC-10Ni Composites

Alexandre Mégret *, Alessandro Magazzu, Véronique Vitry and Fabienne Delaunois

Metallurgy Unit, Faculty of Engineering, Materials Institute, University of Mons, 20 Place du Parc, 7000 Mons, Belgium; alessandro.magazzu@umons.ac.be (A.M.); veronique.vitry@umons.ac.be (V.V.); fabienne.delaunois@umons.ac.be (F.D.)

* Correspondence: alexandre.megret@umons.ac.be

Abstract

Tungsten carbides are important materials for various application fields. Their unique combination of mechanical properties makes them a good choice for applications demanding high hardness and moderate fracture toughness, such as cutting tools, oil and gas, mining, or machining industries. The microstructure is composed of a hard phase embedded in a soft, ductile binder. Cobalt, which provides the best compatibility with the tungsten carbide phase, is the main binder. However, some issues have been addressed to cobalt during the last decades, including a classification as a critical raw material by the European Commission, a fluctuation of its price due to intense use in batteries, and health and ethical problems. Nickel-based binders are thus a good alternative to cobalt. Nevertheless, their processing requires a higher sintering temperature to achieve full density, which leads to abnormal grain growth and thus reduces mechanical properties. The proposed solution is to use a small amount of boron, which is added during the milling of the powders, to reduce the sintering temperature. After vacuum sintering, the results show that the sintering temperature can be decreased to reach full density. Mechanical properties show enhanced hardness with moderately decreased fracture toughness compared to the parts without boron additions (hardness around 1450 to 1515 HV_{30} and fracture toughness around 10 to 12 MPa$\sqrt{m}$). Those results provide a good hardness-to-toughness ratio.

Keywords: WC-Ni; boron additions; CalPhaD; alternative binder; mechanical properties

1. Introduction

Cemented carbides are high-performance materials that are used in various applications such as cutting tools (metal cutting inserts, wood knives), mining tools (drilling heads, shearers' teeth), and wear parts (dies, milling bowls) [1]. Their use is strongly dependent on their mechanical properties, which are given by the combination of a hard phase and a soft, ductile metallic binder. The microstructure of the composite provides an excellent hardness-to-toughness ratio and great wear and corrosion resistance in comparison to other conventional cutting tools, for instance [2–6].

Cobalt-based binders are widely used in the hardmetal industry due to their excellent compatibility with the carbide phase. The advantages of cobalt include the formation of a eutectic at low temperature (around 1320 °C), the high solubility of tungsten in cobalt, and the good wettability of the molten cobalt around the carbide particles. All those parameters are essential for the powder metallurgy processing route that is composed of

Academic Editor: Paul F. Luckham

Received: 20 March 2026
Revised: 2 June 2026
Accepted: 3 June 2026
Published: 9 June 2026

milling of the different powders, followed by the shaping of the green bodies and liquid phase sintering [7–10].

However, the use of cobalt in hardmetals is nowadays controversial due to different factors: (a) its scarcity for the EU because most of the cobalt mines are found in the Republic Democratic of the Congo (cobalt has been listed as critical raw material by the European Commission since 2011 [11,12]), (b) its price increase because of the massive use of cobalt for batteries in electrical vehicules [12], and (c) the toxicity of cobalt powders [13,14]. A lot of research has been undertaken to find an alternative to cobalt [15,16]. Among the candidates, nickel is a powerful alternative to cobalt in terms of corrosion resistance [17–19] but has some drawbacks. Although the melting temperature of nickel is lower than that of cobalt, the ternary eutectic temperature of the W-C-Ni system is 70 °C higher than that of the W-C-Co system. Consequently, the sintering temperature of nickel-based binder hardmetals is also higher in nickel binders [6,20–23]. Moreover, as the solubility of tungsten is greater in nickel than in cobalt, nickel-based binders induce larger grain growth during sintering [18,24].

A solution to limit the sintering temperature and thus to reduce the grain growth during sintering is the use of a chemically activated liquid phase sintering. A small content of an element that can form a eutectic at a lower temperature than the melting of the binder is incorporated during the mixing of the powders [25–27]. Nickel-boron alloy, which has been widely studied in various application fields (especially in coatings [28,29]), is known for its eutectic at a much lower temperature (1093 °C) than the WC-Ni eutectic (Figure 1). A previous study that was conducted on the use of boron-cobalt binder in recycled WC-Co showed interesting results where the sintering temperature could be decreased by 100 °C without modification of the density and mechanical properties [30]. The present paper proposes a study of the sintering of tungsten carbide-based materials bound with Ni-B alloy. The influence of the boron content on mechanical properties will be undertaken.

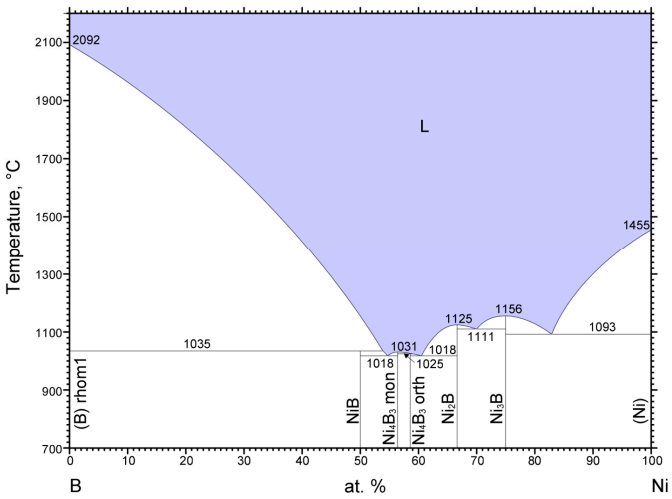

Figure 1. Ni-B binary phase diagram [31]. Reprinted with permission of ASM International. All rights reserved.

2. Materials and Methods

The composite WC-Ni-B powders have been prepared by a two-step ball milling as in previous studies [32,33]. First, the nickel powder (Sigma-Aldrich, Saint-Louis, MO, USA, 3 µm average particle size, 99.7%) and the boron powder (Merck, Darmstadt, Germany, 99%) have been milled in ethanol for 10 h of effective milling at 600 rpm. Four batches at different boron contents have been made (0, 1, 2 and 3 wt.%). Those values have been chosen to have the best efficiency of the boron: indeed, the eutectic at 1093 °C (Figure 1)

limits the maximum amount of boron addition to 18 at.% (3.5 wt.%). Then, the boron-doped nickel powders have been milled with tungsten carbide powder (Wolfram Bergbau und Hütten, Mittersill, Austria, 1 µm average particle size) for 6 h in ethanol at 300 rpm to form WC-10wt.%Ni powders (the composite powders contain 0, 0.1, 0.2 and 0.3 wt.% of boron). The samples will be named WC-10Ni, WC-10(Ni-1B), WC-10(Ni-2B) and WC-10(Ni-3B) respectively. No grain growth inhibitors have been used. All millings have been carried out with a Fritsh Pulverisette 7 Premium Line Planetary Ball Mill (Idar-Oberstein, Germany) equipped with tungsten carbide bowls and balls. The composite powders have then been shaped by uniaxial pressing (500 MPa, sample size 10 mm in diameter and a few millimetres in thickness) before sintering in vacuum (pressure lower than 10^{-3} MPa). The sintering has been carried out at four different temperatures (1375 °C, 1400 °C, 1425 °C, and 1450 °C) for 1 h in a ThermConcept tubular furnace (Hemelingen, Germany). The heating and cooling rates are 4 °C/min. All sintering conditions have been reproduced three times to ensure the validity of the results.

Porosities have been calculated with the open-source software ImageJ (version 1.53e) at different areas of the samples and have been correlated with the measurement of the relative density realized by Archimedes' principle. The phases and the crystallite size of the powders and sintered parts have been analyzed by X-ray diffraction, using a θ-θ configuration device equipped with a copper anti-cathode, λ = 1.54 Å (Siemens D5000, Munich, Germany). The samples have been cut, mounted into resin, and then polished. Murakami etchant (5 g $K_3[Fe(CN)]_6$, 5 g NaOH, 100 mL distilled water) has been used to reveal the microstructure. Optical (Leica, Wetzlar, Germany) and scanning electron (HITACHI SU8020, Tokyo, Japan) microscopes have been used to acquire microstructures. The grain size distribution has been determined by the linear intercept method from the SEM images. The analysis of grain size distributions has been achieved with the characterization of more than 500 WC grains for each set of chemical composition and sintering temperature.

Mechanical properties have been characterized from macro-Vickers hardness (EMCO-Test M4U-025 device, Kuchl, Austria) under 30 kgf load and fracture toughness using the Palmqvist Equation (1).

$$K_{1c} = A\sqrt{\frac{HV_{30}}{\sum l}} \quad (1)$$

where K_{1c} is the stress intensity factor (MPa$\sqrt{m}$), A is a constant (A = 0.15 if hardness is realized with a Vickers indenter under 30 kgf), HV_{30} is the Vickers macro-hardness under 30 kg load (HV_{30}), and $\sum l$ is the sum of the cracks (mm) that appeared at the corners of the print.

Thermodynamical assessment was achieved with Thermo-Calc software (version 2022b, Solna, Sweden) using the TCFE11 Steel and Fe-alloys database. Pseudo-binary phase diagrams with fixed binder contents of 10 wt.% were generated to evaluate the compatibility between the binder and the carbide phase.

3. Results

Phase diagrams have been generated with Thermo-Calc (TCFE11 database) and are displayed in Figure 2. According to the thermodynamical modelling, boron additions have two effects on the phase formation. As stated by the literature review, the liquidus temperature decreases with boron additions. Sintering at a lower temperature is thus possible thanks to the formation of a eutectic transformation between nickel and boron. The second effect is a shift in the graphite stability toward higher carbon contents, which is extremely interesting because graphite must be avoided in cemented carbides due to its harmful effects on the mechanical properties. Some phases containing $(Ni,W)_3B$ and

$(Ni,W)_2B$ might be formed, but their amount is really low due to the low percentage of boron that is used. The effect of those phases on the mechanical properties can thus be neglected. A higher amount of boron is thus preferential since it decreases the sintering temperature and avoids the formation of the graphite phase without forming the η-phase. The latter phase is a brittle carbide with the generic formula M_6C, which has the tendency to highly decrease the fracture toughness. It is thus preferable to also avoid this η-phase.

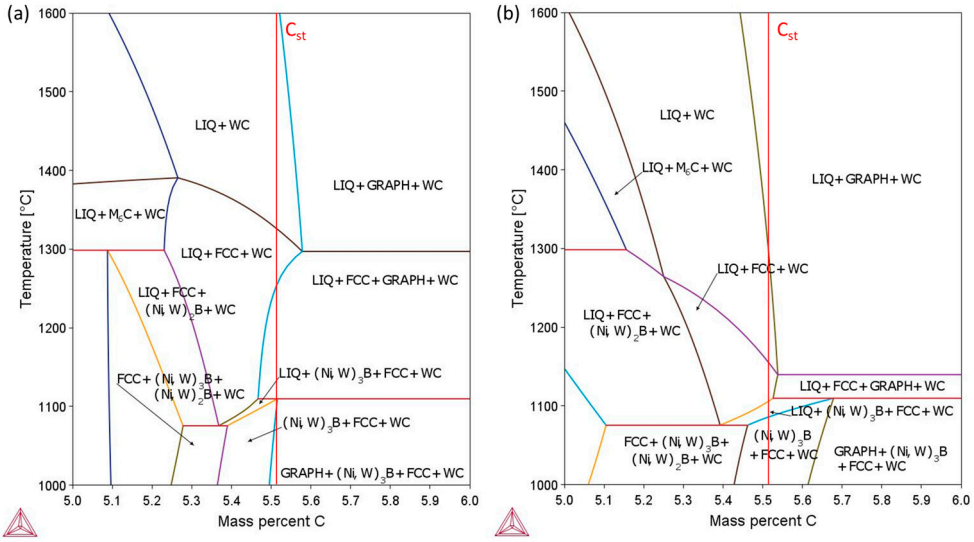

Figure 2. Pseudo-binary W-C-Ni-B phase diagrams with fixed binder amount and compositions: (**a**) WC-10(Ni-1B), (**b**) WC-10(Ni-3B).

Figure 3 shows the evolution of the porosity of the samples as a function of the temperature and boron additions. With no boron additions, the density is high, but the samples contained large porosities with an average size higher than 10 µm (type B). At low temperature (1375–1400 °C), both WC-10Ni and WC-10(Ni-1B) samples showed high porosity content. The amount of boron is not sufficient to reach a good liquid spreading around the carbide, and thus, the densities of the samples are lower. From 0.2 to 0.3 wt.% boron in the composite powder, it is shown that the porosity content is low and will remain more or less constant with decreasing temperature. At 1425–1450 °C, the samples containing 0 and 0.1 wt.% boron show a decrease in their porosity contents. In these cases, the higher temperatures create higher liquid amounts, and thus a better sinterability. The relative densities measured by Archimedes' principle are in good agreement with the measures of the porosity. The relative density of WC-10Ni parts is low at 1375 °C (92%) and increases with the increase in the sintering temperature to reach 99% at 1450 °C. The parts containing 0.1 wt.% boron in the composite powder have relative densities around 95% at low sintering temperatures. The relative densities of boron-doped parts (0.1 wt.% boron from 1425 °C, and 0.2 and 0.3 wt.% boron are all above 99%).

Grain size distributions are provided in Figure 4: it is clearly seen that the addition of boron promotes grain growth during sintering, as shown by arrows on the graphs. This is probably linked to the formation of a liquid at a lower temperature than the conventional sintering temperature because the WC grain growth is governed by the solution-reprecipitation process. As that process is diffusion-dependent [34], larger WC grains are expected for higher sintering temperatures or higher boron contents.

Without boron additions, the average grain size is thus low, around 650–720 nm, with only a few WC grains larger than 2 µm. Their grain size distributions are also narrower. The 0.3 wt.% boron samples admit larger grains, with many grains between 3 and 5 µm.

With increasing temperature, larger WC grains are observed due to the higher diffusion rates that govern the liquid-phase sintering of cemented carbides.

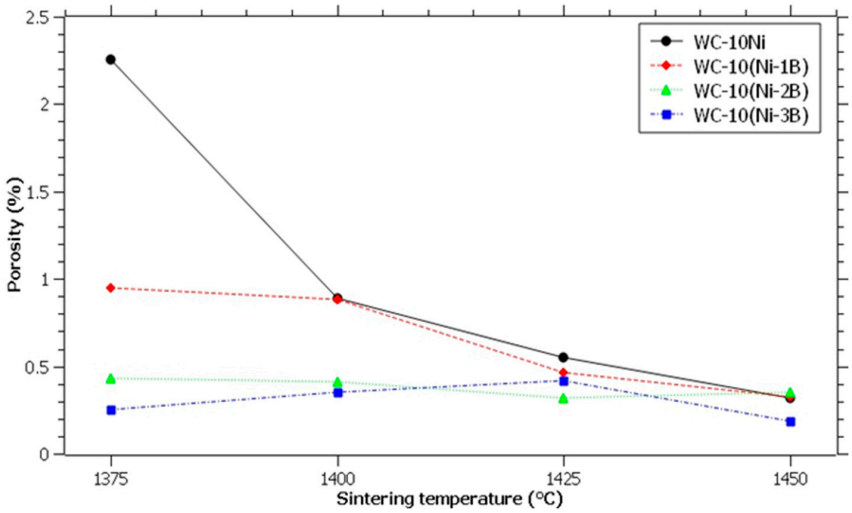

Figure 3. Evolution of the porosity as a function of the sintering temperature.

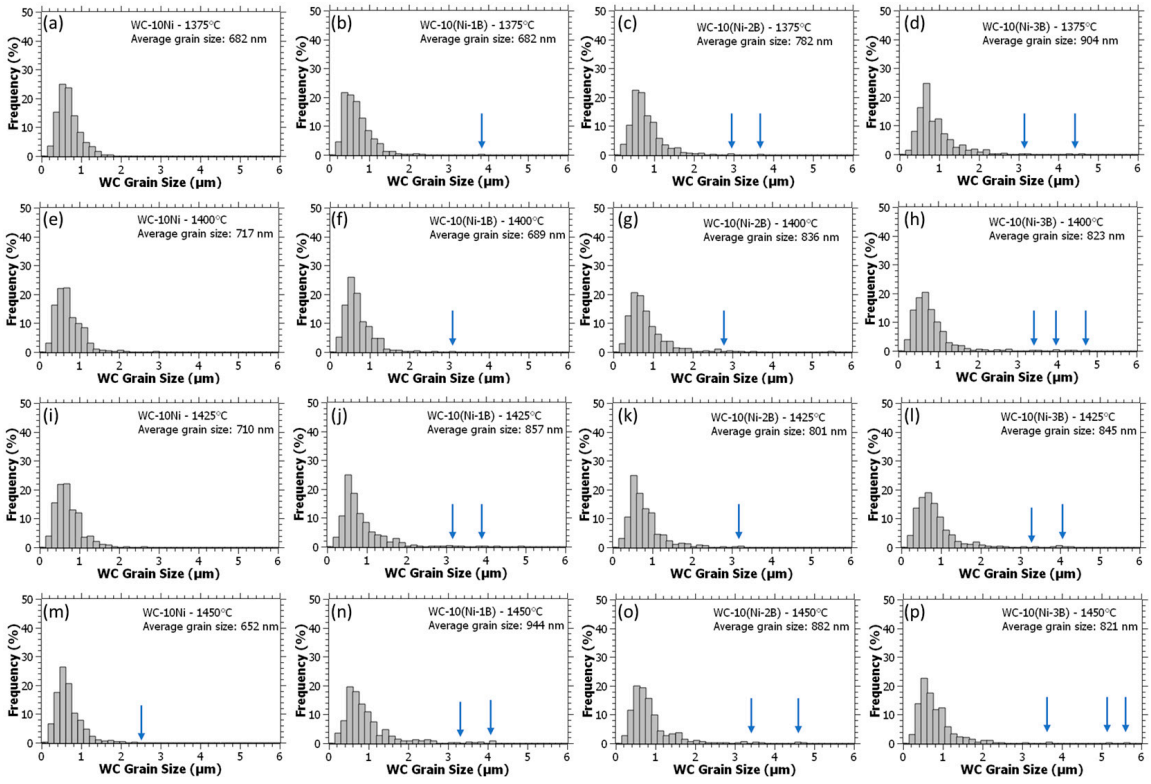

Figure 4. Grain size distributions, calculated based on the analysis of more than 500 WC grains per sample: (**a**) 1375 °C—WC-10Ni, (**b**) 1375 °C—WC-10(Ni-1B), (**c**) 1375 °C—WC-10(Ni-2B), (**d**) 1375 °C—WC-10(Ni-3B), (**e**) 1400 °C—WC-10Ni, (**f**) 1400 °C—WC-10(Ni-1B), (**g**) 1400 °C—WC-10(Ni-2B), (**h**) 1400 °C—WC-10(Ni-3B), (**i**) 1425 °C—WC-10Ni, (**j**) 1425 °C—WC-10(Ni-1B), (**k**) 1425 °C—WC-10(Ni-2B), (**l**) 1425 °C—WC-10(Ni-3B), (**m**) 1450 °C—WC-10Ni, (**n**) 1450 °C—WC-10(Ni-1B), (**o**) 1450 °C—WC-10(Ni-2B), (**p**) 1450 °C—WC-10(Ni-3B).

The hardness properties (Figure 5) depend on two different factors: firstly, higher density (i.e., lower porosity) will induce higher hardness, and secondly, as hardness and WC grain size are linked by the Hall-Petch relationship, the hardness is inversely proportional to the grain size. Hardness measurements are in good agreement with the grain size

distributions. Without boron additions, the hardness remains constant, between 1425 and 1450 $HV_{30,}$ because the grain size distributions and the average grain size are similar. However, a decrease in the sintering temperature to 1425 and 1375 °C shows a lower average hardness with large standard deviations linked with a higher amount of porosity and a less homogeneous microstructure. With increasing the boron content in the binder, the hardness decreases with higher sintering temperature due to the increase in the average grain size and the formation of large WC grains (>4 µm). At low sintering temperature (1375–1400 °C), hardness is higher with boron additions due to the higher densities obtained after sintering (1450–1525 HV_{30}) and narrower grain size distributions. Fracture toughness (Figure 6) does not show a particular trend since standard deviations are high due to higher porosity content in 0 wt.% B samples, and the large WC grains above 3 µm. Fracture toughness values are comprised between 10 and 20 MPa$\sqrt{m}$. At low sintering temperature (1375 °C), fracture toughness is low due to narrow grain size distributions and lower average grain size. In summary, the mechanical properties are consistent with the literature and, in particular, with the work of Chychko et al. [35].

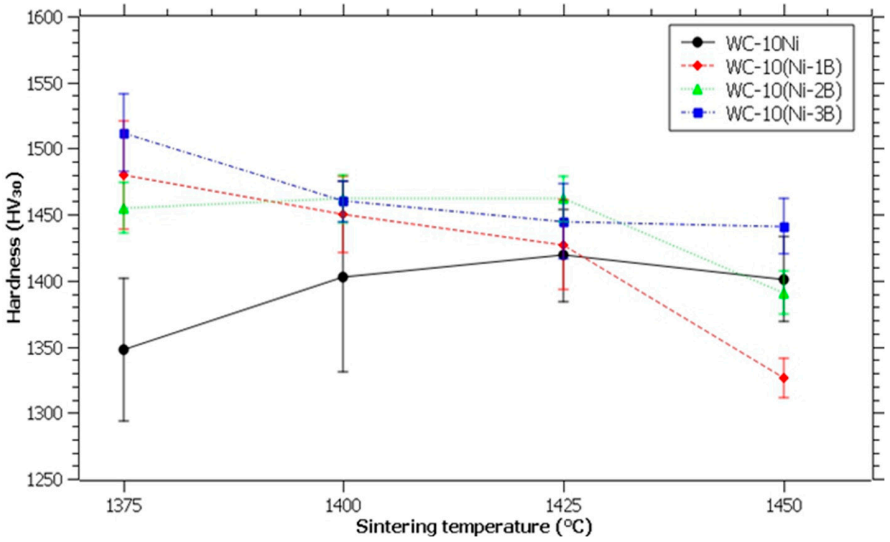

Figure 5. Evolution of hardness as a function of the sintering temperature.

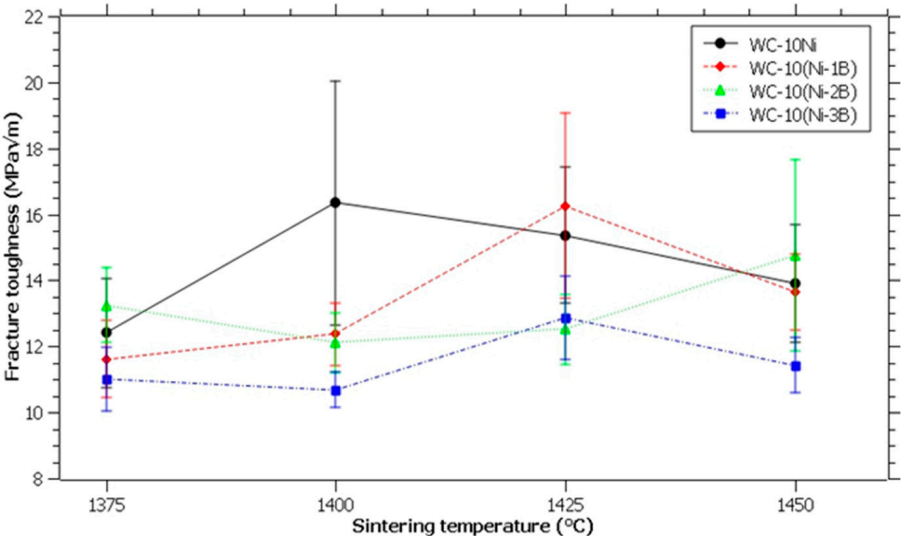

Figure 6. Fracture toughness as a function of the sintering temperature.

4. Discussion

The selection of the optimum sintering temperature has been made by the combined analysis of the porosity and mechanical properties. The standard deviations of hardness and fracture toughness are indeed high for some parts. For boron-free parts, it is explained by the lower relative density of the parts sintered at low temperatures. The presence of type B porosity (size superior to 10 µm) leads to a deviation of the hardness values. From 1425 °C, the standard deviations are lower, a sign that the samples have reached almost full density. For boron- doped parts, the standard deviations of fracture toughness suffer from the disparity of the WC grain size because fracture toughness is greatly influenced by large WC grains. To guarantee consistent mechanical properties, parts sintered at 1375 °C have been selected for further analyses. They are indeed promising because they provide better mechanical properties than the boron-free parts. Despite wider WC grain size distributions, their hardness shows a 10% improvement, mainly due to the higher relative density obtained after sintering, while the fracture toughness is comparable to that of boron-free parts. Moreover, sintering at a lower temperature is preferable for energy saving.

X-ray diffraction and microstructure evaluation have thus been achieved on the parts sintered at 1375 °C. Figure 7 shows the X-ray diffractograms of the samples sintered at 1375 °C for 1 h. As suggested by thermodynamical modelling, no graphite phase was formed during the sintering of the parts. Moreover, only WC and Ni phases are observed and not the $(Ni,W)_3B$ phase, suggesting that their proportions are really small in the microstructures. XRD patterns thus show appropriate phases for mechanical investigation. The microstructures shown in Figure 8 are homogeneous in terms of WC grain size and phase distributions. Without boron, nickel pools are observed due to the lower amount of liquid available at the sintering temperature. On the other hand, the parts containing boron do not show any nickel pools thanks to the eutectic liquid between boron and nickel. Even if it is not shown in the XRD patterns, the sample without boron additions admits large porosities that could be residues of graphite precipitation. Figure 9 shows low and high-magnification images of the parts sintered at 1375 °C. The distribution of nickel in the boron-doped parts is better than in the boron-free part, as indicated by the formation of nickel pools in part WC-10Ni (Figure 9a,b). The promotion of large WC grains is clearly observed for the boron-doped samples (Figure 9c–h).

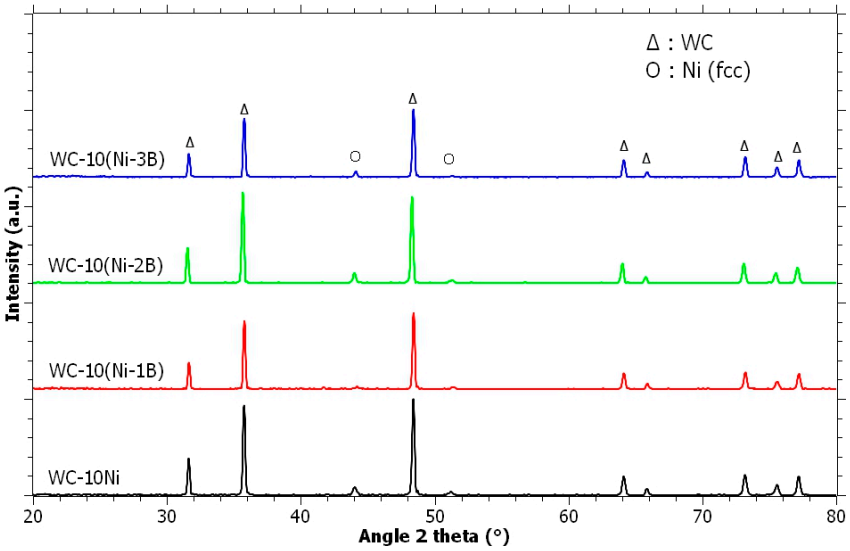

Figure 7. X-ray diffraction of the powders sintered at 1375 °C: WC-10Ni, WC-10(Ni-1B), WC-10(Ni-2B), WC-10(Ni-3B).

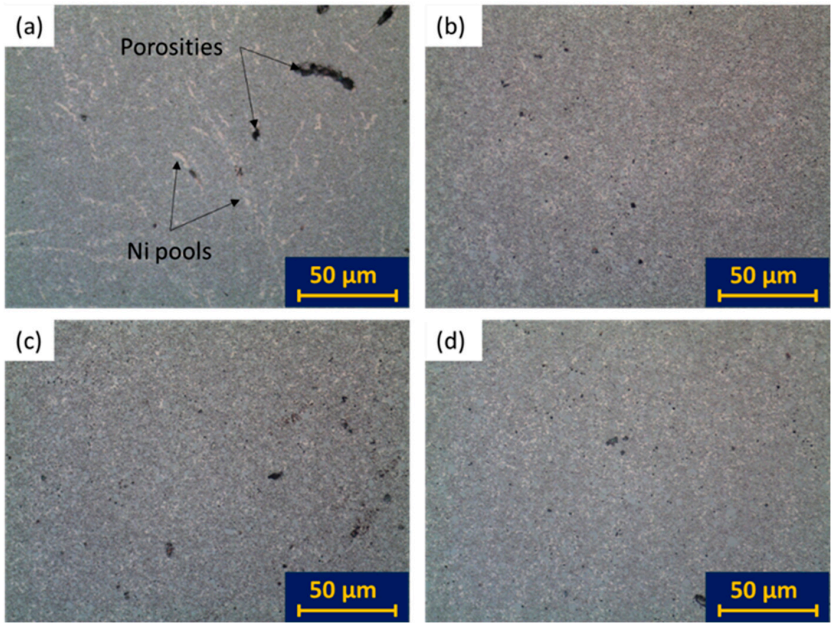

Figure 8. Optical microstructures of the parts sintered at 1375 °C: (**a**) WC-10Ni, (**b**) WC-10(Ni-1B), (**c**) WC-10(Ni-2B), (**d**) WC-10(Ni-3B).

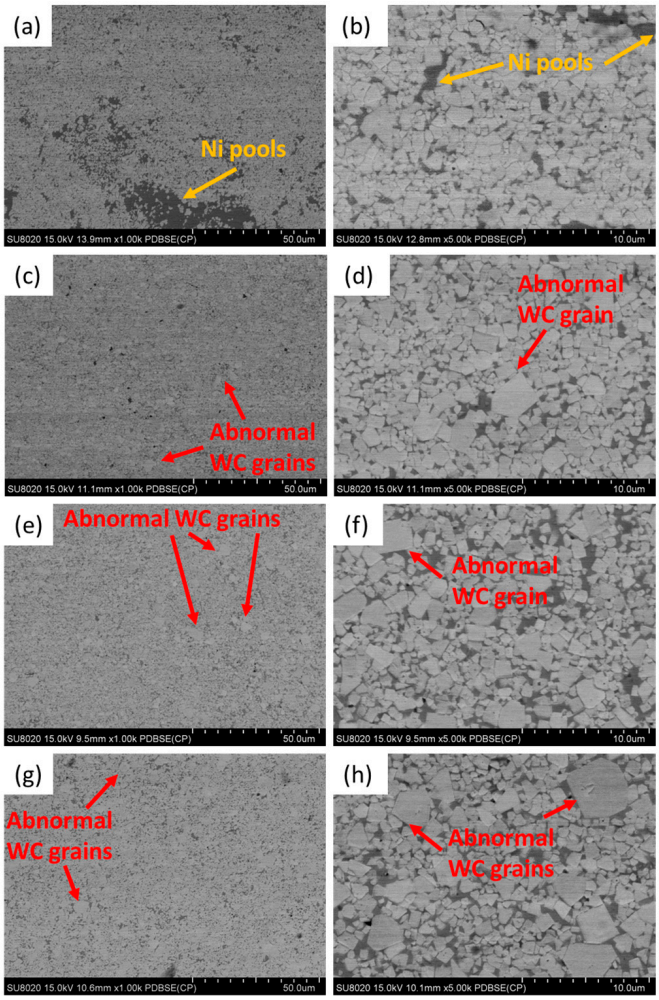

Figure 9. SEM (backscattered electrons images) microstructures of the parts sintered at 1375 °C: (**a**,**c**,**e**,**g**) low magnification, ×1000, (**b**,**d**,**f**,**h**) high magnification, ×5000 (**a**,**b**) WC-10Ni, (**c**,**d**) WC-10(Ni-1B), (**e**,**f**) WC-10(Ni-2B), (**g**,**h**) WC-10(Ni-3B).

In the paper of Chychko et al. [35], HV-K_{IC} properties maps of cemented carbides with different binders are plotted. According to their plots, the parts of this work (Vickers hardness of 1450–1550 HV_{30} and fracture toughness 10–14 MPa$\sqrt{m}$) are situated in the average values for WC-10Co and in the top values for WC-10Ni. Compared to a previous publication [32], the hardness of the WC-10Ni(B) is, however, lower than that of WC-10Co (1715 ± 15 HV_{30}), while the fracture toughness is slightly enhanced (10.7 ± 0.8 MPa$\sqrt{m}$). In summary, the properties of boron-doped WC-10Ni(B) composites are in good agreement with the required properties of cutting tools or cutting inserts operating at low temperature and low cutting speed [36].

5. Conclusions

The analysis of the mechanical properties shows that the hardness is strongly affected by the relative density, while the fracture toughness is more affected by the WC grain size distribution, and in particular by larger grains. The sintering temperature has been selected to enhance the homogeneity of the microstructures and to decrease the dispersion of the mechanical properties.

With small amounts of boron, the sintering temperature of cemented tungsten carbide-nickel was decreased. Full density was achieved at 1375 °C for parts containing 0.2 and 0.3 wt.% boron in the composite powder. No graphite precipitation was observed in the microstructure or in the XRD patterns. The microstructures are also more homogeneous, without the presence of nickel concentrations, which are usually responsible for poor mechanical properties. Although the addition of boron promoted WC grain growth during conventional vacuum sintering, the mechanical properties, such as hardness, have not been affected. Fracture toughness has slightly decreased compared to higher sintering temperature but is of the same order of magnitude as WC-10Ni sintered at 1375 °C (boron-free part).

The measured mechanical properties and the observed microstructure are thus consistent with use in cutting applications operating at low temperature and/or at low cutting speed.

Author Contributions: Conceptualization, A.M. (Alexandre Mégret), V.V. and F.D.; methodology, A.M. (Alexandre Mégret); software, A.M. (Alexandre Mégret); validation, A.M. (Alexandre Mégret), V.V. and F.D.; investigation, A.M. (Alexandre Mégret) and A.M. (Alessandro Magazzu); data curation, A.M. (Alexandre Mégret), A.M. (Alessandro Magazzu), V.V. and F.D.; writing—original draft preparation, A.M. (Alexandre Mégret); writing—review and editing, A.M. (Alexandre Mégret), A.M. (Alessandro Magazzu), V.V. and F.D.; supervision, V.V. and F.D. All authors have read and agreed to the published version of the manuscript.

Funding: This research was funded by the European Union (European Regional Development Fund-FEDER/Just Transition Fund-FTJ), with the support of Walloon Region (Grant agreement N° 2917, HARDMat).

Institutional Review Board Statement: Not applicable.

Informed Consent Statement: Not applicable.

Data Availability Statement: The original contributions presented in this study are included in the article. Further inquiries can be directed to the corresponding author.

Acknowledgments: The authors acknowledge Wolfram Bergbau une Hütten for providing the WC powder and Materia Nova for SEM analysis.

Conflicts of Interest: The authors declare no conflicts of interest.

References

1. Prakash, L.J. Application of fine grained tungsten carbide based cemented carbides. *Int. J. Refract. Met. Hard Mater.* **1995**, *13*, 257–264. [CrossRef]
2. García, J.; Ciprés, V.C.; Blomqvist, A.; Kaplan, B. Cemented carbide microstructures: A review. *Int. J. Refract. Met. Hard Mater.* **2019**, *80*, 40–68. [CrossRef]
3. Konyashin, I.; Ries, B. *Cemented Carbides*; Elsevier: Amsterdam, The Netherlands, 2022.
4. Upadhyaya, G.S. Materials science of cemented carbides—An overview. *Mater. Des.* **2001**, *22*, 483–489. [CrossRef]
5. Schwarzkopf, P.; Kieffer, R.; Leszynski, W.; Benesovsky, F. *Cemented Carbides*; The MacMillan Company: New York, NY, USA, 1960.
6. von Spalden, M.; Pötschke, J.; Michaelis, A. Novel Alternative Ni-Based Binder Systems for Hardmetals. *Crystals* **2024**, *14*, 1013. [CrossRef]
7. Andren, H.-O. Microstructures of cemented carbides. *Mater. Des.* **2001**, *22*, 491–498. [CrossRef]
8. Snowball, R.F.; Milner, D.R. Densification Processes in the Tungsten Carbide-Cobalt System. *Powder Metall.* **1968**, *11*, 23–40. [CrossRef]
9. Meredith, B.; Milner, D.R. Densification mechanisms in the tungsten carbide-cobalt system. *Powder Metall.* **1976**, *19*, 38–45. [CrossRef]
10. Fang, Z.Z.; Maheshwari, P.; Wang, X.; Sohn, H.Y.; Griffo, A.; Riley, R. An experimental study of the sintering of nanocrystalline WC-Co powders. *Int. J. Refract. Met. Hard Mater.* **2005**, *23*, 249–257. [CrossRef]
11. European Commission. *Tackling the Challenges in Commodity Markets and on Raw Materials*; European Commission: Brussels, Belgium, 2011. [CrossRef]
12. U.S. Geological Survey (USGS). *Mineral Commodity Summaries 2018*; U.S. Geological Survey (USGS): Reston, VA, USA, 2018.
13. Lasfargues, G.; Lison, D.; Maldague, P.; Lauwerys, R. Comparative study of the acute lung toxicity of pure cobalt powder and cobalt-tungsten carbide mixture in rat. *Toxicol. Appl. Pharmacol.* **1992**, *112*, 41–50. [CrossRef]
14. Bastian, S.; Busch, W.; Kühnel, D.; Springer, A.; Meißner, T.; Holke, R.; Scholz, S.; Iwe, M.; Pompe, W.; Gelinsky, M.; et al. Toxicity of tungsten carbide and cobalt-doped tungsten carbide nanoparticles in mammalian cells in vitro. *Environ. Health Perspect.* **2009**, *117*, 530–535. [CrossRef]
15. Molla, T.T.; Jonsson, C.O.; Schaffer, G. Computational Design of Alternative Binders for Sintering of Tungsten Carbide (WC) Hard Metals. *Integr. Mater. Manuf. Innov.* **2025**, *14*, 153–169. [CrossRef]
16. Kurbanbekov, S.; Kozhakhmetov, Y.; Skakov, M.; Seitov, B.; Aidarova, M.; Tabiyeva, Y. Properties, Advantages, and Prospects of Using Cobalt-Free Composites Based on Tungsten Carbide in Industry. *Materials* **2025**, *18*, 129. [CrossRef]
17. Tomlinson, W.J.; Linzell, C.R. Anodic polarization and corrosion of cemented carbides with cobalt and nickel binders. *J. Mater. Sci.* **1988**, *23*, 914–918. [CrossRef]
18. Tracey, V.A. Nickel in Hardmetals. *Int. J. Refract. Met. Hard Mater. Hard Mater.* **1992**, *11*, 137–149. [CrossRef]
19. Chang, S.H.; Chen, S.L. Characterization and properties of sintered WC-Co and WC-Ni-Fe hard metal alloys. *J. Alloys Compd.* **2014**, *585*, 407–413. [CrossRef]
20. Wittmann, B.; Schubert, W.D.; Lux, B. WC grain growth and grain growth inhibition in nickel and iron binder hardmetals. *Int. J. Refract. Met. Hard Mater.* **2002**, *20*, 51–60. [CrossRef]
21. Shi, K.H.; Zhou, K.C.; Li, Z.Y.; Zhang, D.; Zan, X.Q. Microstructure and formation process of Ni-pool defect in WC-8Ni cemented carbides. *Trans. Nonferrous Met. Soc. China (Engl. Ed.)* **2015**, *25*, 873–878. [CrossRef]
22. Phuong, D.D.; Van Trinh, P.; Van Duong, L.; Chung, L.D. Influence of sintering temperature on microstructure and mechanical properties of WC-8Ni cemented carbide produced by vacuum sintering. *Ceram. Int.* **2016**, *42*, 14937–14943. [CrossRef]
23. Shon, I.J.; Jeong, I.K.; Ko, I.Y.; Doh, J.M.; Woo, K.D. Sintering behavior and mechanical properties of WC-10Co, WC-10Ni and WC-10Fe hard materials produced by high-frequency induction heated sintering. *Ceram. Int.* **2009**, *35*, 339–344. [CrossRef]
24. Steinlechner, R.; de Oro Calderon, R.; Koch, T.; Linhardt, P.; Schubert, W.D. A study on WC-Ni cemented carbides: Constitution, alloy compositions and properties, including corrosion behaviour. *Int. J. Refract. Met. Hard Mater.* **2022**, *103*, 105750. [CrossRef]
25. Upadhyaya, G.S. Some issues in sintering science and technology. *Mater. Chem. Phys.* **2001**, *67*, 1–5. [CrossRef]
26. Zhang, F.; Shen, J.; Sun, J. The effect of phosphorus additions on densification, grain growth and properties of nanocrystalline WC-Co composites. *J. Alloys Compd.* **2004**, *385*, 96–103. [CrossRef]
27. Zovas, P.E.; German, R.M.; Hwang, K.S.; Li, C.J. Activated and Liquid-Phase Sintering-Progress and Problems. *J. Miner. Met. Mater. Soc.* **1983**, *35*, 28–33. [CrossRef]
28. Vitry, V.; Hastir, J.; Mégret, A.; Yazdani, S.; Yunacti, M.; Bonin, L. Recent advances in electroless nickel boron coatings. *Surf. Coat. Technol.* **2022**, *429*, 127937. [CrossRef]
29. Delaunois, F.; Vitry, V.; Bonin, L. *Electroless Nickel Plating: Fundamentals to Applications*; CRC Press: Boca Raton, FL, USA, 2019.
30. Mégret, A.; Vitry, V.; Delaunois, F. The effect of boron-doped cobalt additions on mechanical properties of a recycled WC-Co powder. *Int. J. Refract. Met. Hard Mater.* **2023**, *111*, 106098. [CrossRef]

31. Okamoto, H.; Schlesinger, M.E.; Mueller, E.M. (Eds.) *ASM Handbook, Volume 3: Alloy Phase Diagrams*; ASM International: Almere, The Netherlands, 2016.
32. Mégret, A.; Vitry, V.; Delaunois, F. High-energy ball milling of WC-10Co: Effect of the milling medium and speed on the mechanical properties. *Int. J. Refract. Met. Hard Mater.* **2022**, *104*, 105774. [CrossRef]
33. Stanciu, V.I.; Vitry, V.; Delaunois, F. Influence of the milling parameters on the sintering behaviour of WC-Co composites. *Mater. Manuf. Process.* **2020**, *35*, 811–816. [CrossRef]
34. German, R.M.; Farooq, S.; Kipphut, C.M. Kinetics of Liquid Phase Sintering. *Mater. Sci. Eng. A* **1988**, *105–106*, 215–224. [CrossRef]
35. Chychko, A.; García, J.; Ciprés, V.C.; Holmström, E.; Blomqvist, A. HV-KIC property charts of cemented carbides: A comprehensive data collection. *Int. J. Refract. Met. Hard Mater.* **2022**, *103*, 105763. [CrossRef]
36. Schneider, G. *Cutting Tools Applications*; ASM International: Almere, The Netherlands, 2002.